Share Your Innovations through JACS Directory

Journal of Nanoscience and Technology

Visit Journal at http://www.jacsdirectory.com/jnst

ISSN: 2455-0191

Spectroscopic and Morphological Behavior of Co_3O_4-MnO_2-ZrO_2 Ternary Nanoparticles

S. Alwin David, V. Veeraputhiran, C. Vedhi*

Department of Chemistry, V.O. Chidambaram College, Tuticorin – 628 008, Tamil Nadu, India.

ARTICLE DETAILS

Article history:
Received 11 November 2017
Accepted 27 November 2017
Available online 06 December 2017

Keywords:
Co_3O_4-MnO_2-ZrO_2 NPs
Mixed Nano Oxides
Morphology
Spectroscopy

ABSTRACT

Co_3O_4-MnO_2-ZrO_2 mixed oxides nanoparticles were formed when aqueous solution of cobalt chloride, manganese (II) sulfate and zirconium oxychloride and sodium hydroxide is refluxed at elevated temperature. The spectroscopic and morphological behavior of mixed nano oxides were studied by FT-IR, XRD, UV – Vis DRS, TEM, SAED, SEM, EDAX and AFM. The presence of M-O bonds (M = Co, Mn, Zr) was confirmed by FTIR spectra. XRD studies revealed that the size of the Co_3O_4-MnO_2-ZrO_2 NPs is in the range of 32.87 – 59.13 nm. Band gap energies of the (0.1 – 0.5 M) Co_3O_4-MnO_2-ZrO_2 NPs were found to be in the range of 2.27 – 2.37 eV as evident from UV-Vis diffuse reflectance spectra (DRS). The TEM, SEM and AFM micrographs of 0.1 M Co_3O_4-MnO_2-ZrO_2 NPs exhibited roughly spherical shape with size ranging from 30 – 80 nm. SAED pattern confirmed the crystalline nature of Co_3O_4-MnO_2-ZrO_2 NPs. EDAX analysis exposed the presence of Co, Mn, Zr and O.

1. Introduction

In the universe there are huge number of metal oxides are existing in nature but some of the metal oxides are most useful in accordance with their applications in science and technology. In the periodic table transition metals are large in number and have number of applications in different fields. Some transition metal oxides like Co_3O_4, MnO_2, and ZrO_2 etc proved as potential candidates for so many applications [1-6]. Recently, there has been increasing interest in the synthesis of nanocrystalline mixed metal oxides. Among the transition metal oxides, cobalt oxide (Co_3O_4) is one of the most significant materials because of its thermal stability and attractive properties. The Co_3O_4 is a p-type semiconducting materials with chemical stability at high temperature and high mechanical strength [1, 2].

Manganese oxide exhibits various forms like MnO, MnO_2, Mn_2O_3, Mn_3O_4 and Mn_5O_8. In which, MnO_2 is one of the most attractive oxide with low band gap, high optical constant, ferroelectric and catalytic properties [3, 4].

Zirconia (ZrO_2) is a chemically inert substance; it has excellent corrosion resistance in acids and alkalis. Another exceptional property of ZrO_2 is stability under reducing environment, which makes it as a significant material in catalytic field [5, 6].

In this paper, synthesis of Co_3O_4-MnO_2-ZrO_2 NPs and their spectroscopic and morphological behavior are presented. The spectroscopic and morphological behavior of Co_3O_4-MnO_2-ZrO_2 NPs were investigated by FT-IR, XRD, DRS, TEM, SAED, SEM, EDAX, and AFM.

2. Experimental Methods

2.1 Materials

The precursors $CoCl_2.6H_2O$, $MnSO_4.H_2O$, $ZrOCl_2.8H_2O$ and the precipitant (NaOH) were purchased from Merck. All solutions were prepared using deionized water.

2.2 Synthesis of Co_3O_4-MnO_2-ZrO_2 Nanoparticles

About 25 mL of 0.1 M $CoCl_2.6H_2O$ was added to the aqueous solution of 75 mL of 1.0 M NaOH solution and stirred well. To this mixture 25 mL of 0.1 M $MnSO_4.H_2O$ and 25 mL of 0.1 M $ZrOCl_2.8H_2O$ were added. The resulting mixture was stirred well and refluxed at an elevated temperature for 3 hours. The product was filtered, washed with water and dried. Similar procedure was carried out to synthesize different concentrations of (0.2 M - 0.5 M) Co_3O_4-MnO_2-ZrO_2 nanoparticles.

2.3 Characterization

FTIR measurements of samples prepared as KBr disks were performed on a Thermo Scientific Nicolet iS5 FTIR spectrometer. The average particle size of nanoparticles was determined by XPERT-PRO X-ray diffractometer using CuKα radiation. UV-Vis diffuse reflectance spectra were recorded with Jasco V-600 spectrophotometer. Philips-CM200 Transmission Electron Microscopy (TEM) was used to study the shape, particle size and lattice image of the nanoparticles. The morphology and composition of the nanoparticles were determined by JEOL JSM 6390 Scanning Electron Microscopy (SEM) with EDAX. Atomic force microscopy (AFM) images were recorded on a Nanosurf Easyscan 2 AFM instrument to obtain topographical images of the nanoparticles.

3. Results and Discussion

3.1 FTIR Analysis

FTIR spectra of Co_3O_4-MnO_2-ZrO_2 NPs are shown in Fig. 1. The bands in the finger print region, 583 – 1019 cm^{-1} correspond to the lattice vibration modes of M-O (M = Co, Mn, Zr) [7, 8]. IR bands observed at around 1114 – 1117 cm^{-1} are due to the presence of symmetric stretching of M-O (M = Mn, Zr) [8]. The band that appears at 1384 cm^{-1} in the FTIR spectra indicates the presence of M-O rocking in plane vibration mode (M = Co, Mn, Zr) [9]. The absorption peaks at around 1460 – 1464 cm^{-1} are assigned to the stretching vibration modes of Co–O bond [10].

3.2 XRD Analysis

The XRD behaviour of the Co_3O_4-MnO_2-ZrO_2 NPs are presented in Fig. 2, The X - ray diffraction peaks at 2θ values of 31.38°, 36.85° and 55.53° are attributed to (220), (311) and (422) planes of Co_3O_4 (JCPDS card no. 76-1802) respectively [11]. The diffraction peaks at 2θ values of 38.25° and 44.37° are due to (440) and (202) planes of MnO_2 (JCPDS card no. 44-0142) respectively [4]. The diffraction peaks at 2θ values of 50.47° and 58.71° are assigned to (220) and (311) planes of ZrO_2 (JCPDS card no. 50-1089) respectively [5]. Similar diffraction peaks are also observed in all the samples as given in the figure. The average particle sizes of the Co_3O_4-MnO_2-ZrO_2 NPs as estimated using the Scherer's formula are in the range of 32.87 – 59.13 nm. As the concentration of the precursors increases from 0.1 M to 0.5 M, the size of the nanoparticles also increases proportionately due to agglomeration of the small metal oxide nanoparticles.

*Corresponding Author
Email Address: cvedhi23@gmail.com(C. Vedhi)

2455-0191 / JACS Directory©2017. All Rights Reserved

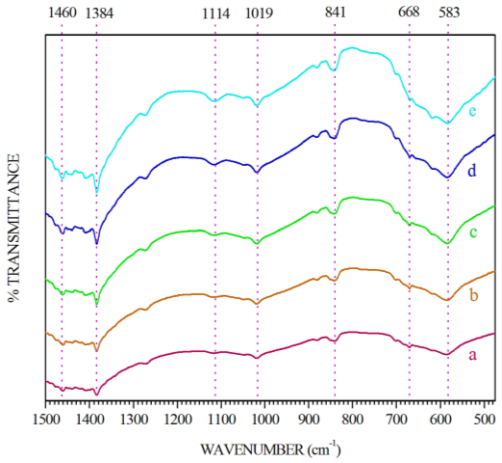

Fig. 1 FTIR Spectra of a) 0.1 M Co_3O_4-MnO_2-ZrO_2 NPs b) 0.2 M Co_3O_4- MnO_2-ZrO_2 NPs c) 0.3 M Co_3O_4- MnO_2-ZrO_2 NPs d) 0.4 M Co_3O_4- MnO_2-ZrO_2 NPs and e) 0.5 M Co_3O_4-MnO_2-ZrO_2 NPs

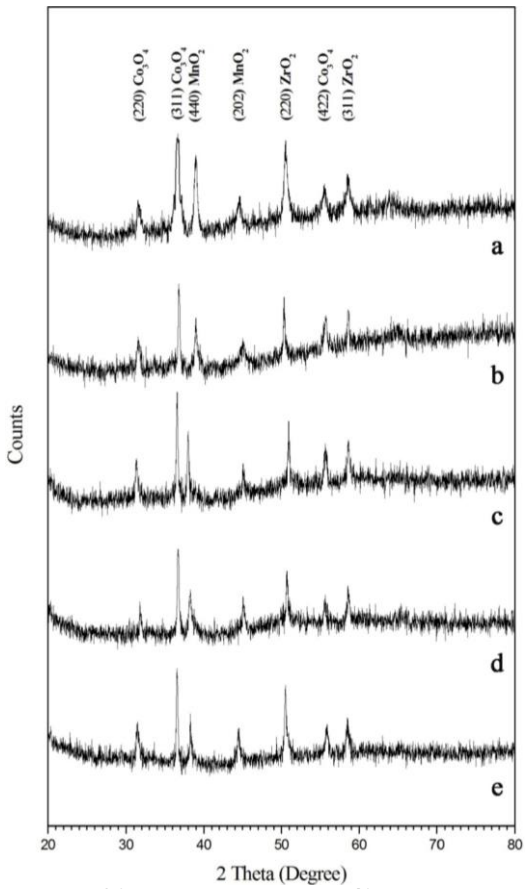

Fig. 2 XRD Patterns of a) 0.1 M Co_3O_4-MnO_2-ZrO_2 NPs b) 0.2 M Co_3O_4- MnO_2-ZrO_2 NPs c) 0.3 M Co_3O_4- MnO_2-ZrO_2 NPs d) 0.4 M Co_3O_4- MnO_2-ZrO_2 NPs and e) 0.5 M Co_3O_4- MnO_2-ZrO_2 NPs

3.3 UV-Visible Diffuse Reflectance Spectroscopic Analysis

The UV-visible absorbance properties of Co_3O_4-MnO_2-ZrO_2 NPs were investigated using UV-Vis diffuse reflectance spectrophotometer in the wavelength range of 200 – 900 nm. As shown in UV-Vis diffuse reflectance spectra (Fig. 3), two absorbance bands centered between 253 - 254 nm and 394 – 403 nm with a hump at around 675 nm, indicate that the samples can be activated by both UV and visible light illumination [11].

There is a red shift in absorption bands (from 394 nm to 403 nm) observed in Co_3O_4-MnO_2-ZrO_2 NPs (from 0.1 M to 0.5 M). This red shift is due to the increase in the particle size as well as decrease in the inter particle distance of Co_3O_4-MnO_2-ZrO_2 NPs (from 0.1 M to 0.5 M) [12].

The band gap (E_g) of the NPs can be determined using well-known Tauc relation, $(\alpha h\nu)^n = A\ (h\nu - E_g)$, where α, h, ν and A are the absorption coefficient, Plank constant, light frequency and a constant, respectively. While n = 2 for direct inter band transition. The Eg value can be estimated by plotting $(\alpha h\nu)^2$ versus $h\nu$ and extrapolating the linear part of curve to energy axis at $\alpha = 0$ (Fig. 4).

The calculated band gap energies are 2.37, 2.36, 2.35, 2.31 and 2.27 eV for 0.1 M, 0.2 M, 0.3 M, 0.4 M and 0.5 M Co_3O_4-MnO_2-ZrO_2 NPs, respectively. The band gap energy values suggest that these Co_3O_4-MnO_2-ZrO_2 NPs are visible light sensitive, capable to be photocatalysts under visible light illumination [11].

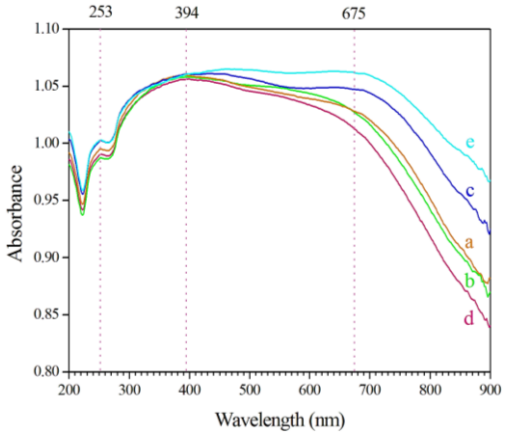

Fig. 3 UV-Visible diffuse reflectance spectra of a) 0.1 M Co_3O_4-MnO_2-ZrO_2 NPs b) 0.2 M Co_3O_4-MnO_2-ZrO_2 NPs c) 0.3 M Co_3O_4-MnO_2-ZrO_2 NPs d) 0.4 M Co_3O_4-MnO_2-ZrO_2 NPs and e) 0.5 M Co_3O_4-MnO_2-ZrO_2 NPs

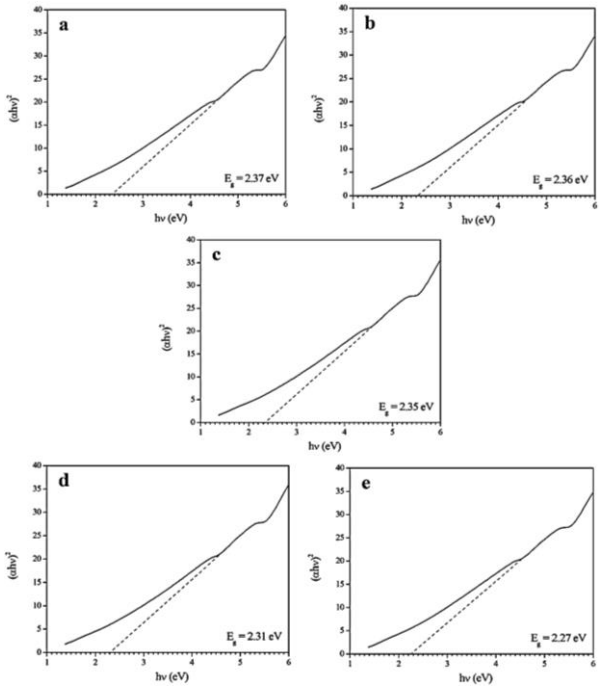

Fig. 4 Plot of $(\alpha h\nu)^2$ versus $(h\nu)$ of a) 0.1 M Co_3O_4-MnO_2-ZrO_2 NPs b) 0.2 M Co_3O_4-MnO_2-ZrO_2 NPs c) 0.3 M Co_3O_4-MnO_2-ZrO_2 NPs d) 0.4 M Co_3O_4-MnO_2-ZrO_2 NPs and e) 0.5 M Co_3O_4-MnO_2-ZrO_2 NPs

3.4 TEM Analysis

TEM images of synthesized Co_3O_4-MnO_2-ZrO_2 NPs are presented in Fig. 5, indicates that the particles are nearly spherical in shape and have average size ranging in between 30–80 nm. The selected area electron diffraction (SAED) pattern of Co_3O_4-MnO_2-ZrO_2 NPs is shown in Fig. 5d. The bright spots on concentric circles in the SAED pattern show the nanocrystalline nature of these nanoparticles.

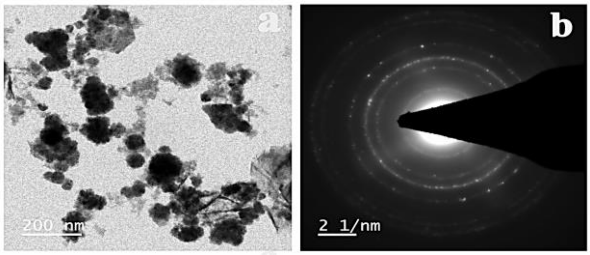

Fig. 5 a) TEM images of 0.1 M Co_3O_4-MnO_2-ZrO_2 NPs and b) SAED pattern of 0.1 M Co_3O_4-MnO_2-ZrO_2 NPs

3.5 SEM Analysis

SEM micrographs of Co_3O_4-MnO_2-ZrO_2 NPs synthesized at five different concentrations of $CoCl_2$, $MnSO_4$ and $ZrOCl_2$ (0.1 M, 0.2 M, 0.3 M, 0.4 M, and 0.5 M) are shown in Figs. 6(a-e). The synthesized Co_3O_4-MnO_2-ZrO_2 NPs exhibits roughly spherical granular morphology with a variety of pores and voids due to the expulsion of large amount of gases that are formed as by product during synthesis [7]. The SEM micrographs also expose that the particle size is significantly increased with increasing concentration of the precursors.

3.6 EDAX Analysis

EDAX mapping was performed to confirm the element distribution in the synthesized Co_3O_4-MnO_2-ZrO_2 NPs. The element mapping of Co, Mn, Zr and O in Fig. 6f directly confirms the formation of Co_3O_4-MnO_2-ZrO_2 NPs. It is very apparent that the sample is free from elemental impurities. Elemental ratio of Co, Mn and Zr obtained from the EDAX spectrum is close to 8.89: 8.87: 11.83 which is in very good agreement with the composition expected from the relative concentrations of Co, Mn and Zr precursors used in the synthesis (1: 1: 1).

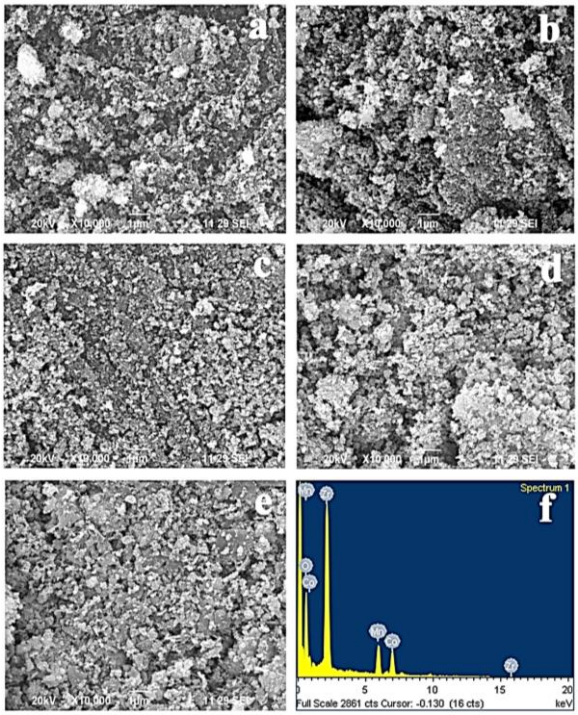

Fig. 6 SEM image of a) 0.1 M Co_3O_4-MnO_2-ZrO_2 NPs b) 0.2 M Co_3O_4-MnO_2-ZrO_2 NPs c) 0.3 M Co_3O_4-MnO_2-ZrO_2 NPs d) 0.4 M Co_3O_4-MnO_2-ZrO_2 NPs and e) 0.5 M Co_3O_4-MnO_2-ZrO_2 NPs

3.7 AFM Analysis

The AFM images illustrate the surface morphology and roughness of Co_3O_4-MnO_2-ZrO_2 NPs are shown in Fig. 7. The shape of Co_3O_4-MnO_2-ZrO_2 NPs is roughly spherical and the size is in the range of 30 – 80 nm.

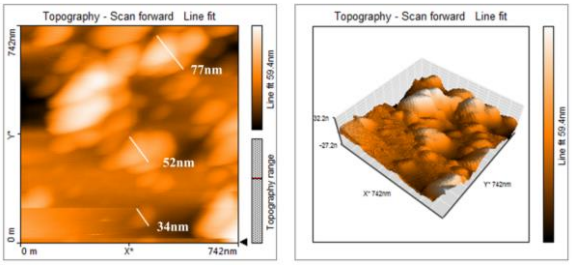

Fig. 7 AFM images of 0.1 M Co_3O_4-MnO_2-ZrO_2 NPs

4. Conclusion

Wet chemical method was used to synthesize Nano Co_3O_4-MnO_2-ZrO_2 mixed oxides. TEM, SEM and AFM micrographs showed that Co_3O_4-MnO_2-ZrO_2 NPs is found to be roughly spherical in shape with size ranging from 30 – 80 nm. From UV-Vis diffuse reflectance spectra (DRS), Band gap energies of the (0.1 – 0.5 M) Co_3O_4-MnO_2-ZrO_2 NPs were found to be in the range of 2.27 – 2.37 eV. The above properties make this Co_3O_4-MnO_2-ZrO_2 NPs suitable for photocatalyst.

References

[1] Y. Wang, W. Wang, W. Song, Binary CuO/Co_3O_4 nanofibers for ultrafast and amplified electrochemical sensing of fructose, Electrochim. Acta 56 (2011) 10191-10196.
[2] T.K. Jana, A. Pal, K. Chatterjee, Magnetic and photocatalytic study of Co_3O_4–ZnO nanocomposite, Jour. Alloys Comp. 653 (2015) 338-344.
[3] B.M.P. Kumar, S. Karikkat, R.H. Krishna, T.H. Udayashankara, K.H. Shivaprasad, B.M. Nagabhushana, Synthesis, characterization of nano MnO_2 and its adsorption characteristics over an azo dye, Res. Rev. Jour. Mater. Sci. 2 (2014) 27-31.
[4] S.S. Falahatgar, F.E. Ghodsi, Optical characterization of nanostructured MnO_2 - ZnO thin films prepared from acetate-based sol–gel precursors, Optik. Int. J. Light Elect. Opt. 127 (2015) 1059 - 1065.
[5] N.C.S. Selvam, A. Manikandan, L.J. Kennedy, J.J. Vijaya, Comparative investigation of zirconium oxide (ZrO_2) nano and microstructures for structural, optical and photocatalytic properties, J. Colloid Interf. Sci. 389 (2013) 91-98.
[6] S.Z. Ajabshir, M.S. Niasari, Facile route to synthesize zirconium dioxide (ZrO_2) nanostructures: Structural, optical and photocatalytic studies, Jour. Mol. Liquids 216 (2016) 545-551.
[7] M.A. Subhan, T. Ahmed, Synthesis, characterization and spectroscopic investigations of novel nano multi-metal oxide Co_3O_4-CeO_2-ZnO, Spectrochim. Acta A: Mol. Biomol. Spect. 129 (2014) 377-381.
[8] R.R. Muthuchudarkodi, C. Vedhi, Synthesis and characterization of nano CuO–ZrO_2 mixed oxide, Adv. Mater. Res. 678 (2013) 50-55.
[9] K.J. Arun, A.K. Batra, A. Krishna, K. Bhat, M.D. Aggarwal, P.J.J. Francis, Surfactant free hydrothermal synthesis of copper oxide nanoparticles, Am. Jour. Mater. Sci. 5 (2015) 36-38.
[10] R.A. Tuwirqi, A.A.A. Ghamdi, N.A. Aal, A. Umar, W.E. Mahmoud, Facile synthesis and optical properties of Co_3O_4 nanostructures by the microwave route, Superlattice. Microst. 49 (2011) 416-421.
[11] Y. Wang, L. Zhou, X. Duan, H. Sun, E.L. Tin, W. Jin, S. Wang, Photochemical degradation of phenol solutions on Co_3O_4 nanorods with sulfate radicals, Catal. Today 258 (2015) 576-584.
[12] S.A. David, K.M. Ponvel, M.A. Fathima, S. Anita, J. Ashli, A. Athilakshmi, Biosynthesis of silver nanoparticles by *Momordica charantia* leaf extract: Characterization and their antimicrobial activities, J. Nat. Prod. Plant Resour. 4 (2014) 1-8.